

## CHAPTER IV

### RESULTS AND DISCUSSIONS

The purpose of this present study was to investigate the effect of different pore structures of MCM-41 support on the catalytic activity during copolymer of ethylene/ $\alpha$ -olefin with bimodal MCM-41-supported zirconocene/dMMAO catalyst including support with a distinct bimodal structure may influences on the catalytic activity and molecular weight distribution of copolymer obtained.

#### 4.1 Characterization of supports and catalyst precursors

##### 4.1.1 Characterization of supports with N<sub>2</sub> physisorption

The MCM-41 supports having different pore structures were prepared based on different pretreatment conditions. After preparation of supports, the unimodal MCM-41 support denoted as UMD having the average pore diameter of ca. 2 nm and surface area of 883.5 m<sup>2</sup>/g was obtained as seen in **Table 4.1**. The pore size distribution of the MCM-41 (UMD) is shown in **Figure 4.1** indicating only the unimodal pore size distribution. By treating the MCM-41 (UMD) with *N,N*-dimethyldecylamine at the specified conditions, the bimodal MCM-41 supports denoted as BMD can be achieved. The BMD1 is assigned to the bimodal MCM-41 support having the average pore diameter of ca. 3.2 and 24.4 nm (surface area = 400.3 m<sup>2</sup>/g) whereas the BMD2 refers to the bimodal MCM-41 with the average pore diameter of ca. 3.2 and 48.4 nm (surface area = 400.0 m<sup>2</sup>/g) as also shown in **Table 4.1** and **Figure 4.1**. As seen in **Figure 4.1**, it can be observed that the MCM-41 (BMD2) support exhibited larger portion of the large pore than the MCM-41 (BMD1) one.

**Table 4.1** BET surface area and average pore diameter of various MCM-41 supports

Support	BET surface area (m <sup>2</sup> /g)	Average pore diameter (nm)
MCM-41(UMD)	863.5	2.3
MCM-41(BMD1)	400.3	3.2 , 24.4
MCM-41(BMD2)	400.0	3.2 , 48.4

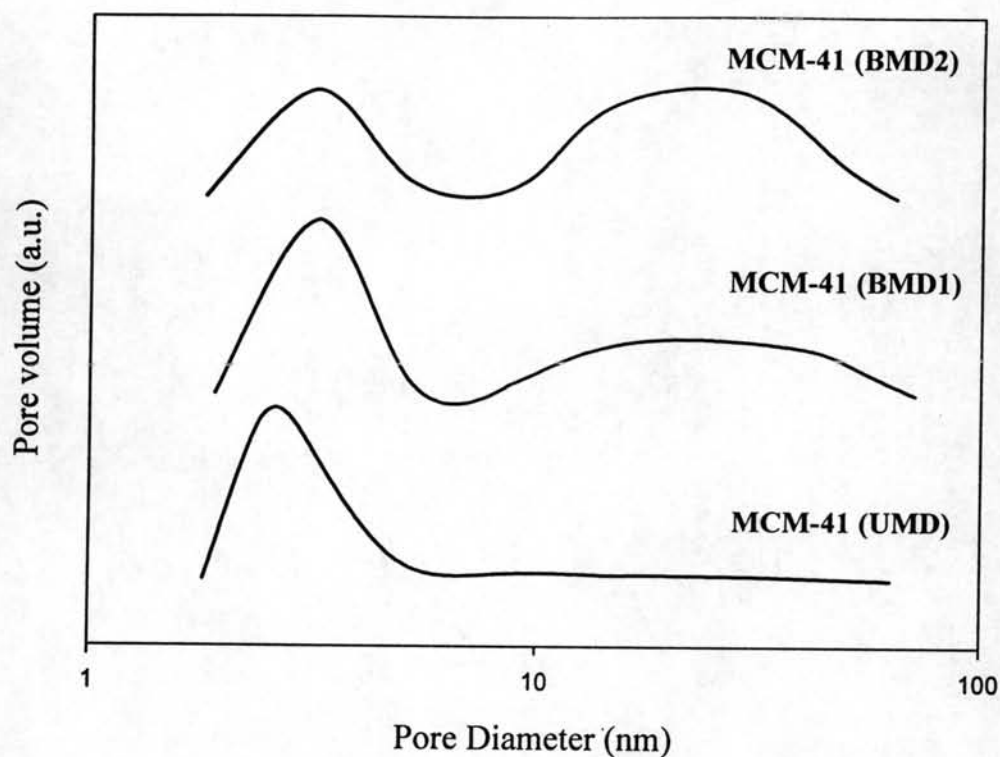


**Figure 4.1** Pore size distribution of various MCM-41 supports

#### **4.1.2 Characterization of supports and catalyst precursors with x-ray diffraction (XRD)**

The various MCM-41 supports with different pore structure were characterized before impregnation with dMMAO. The XRD patterns of MCM-41 supports with different pore structure are shown in **Figure 4.2**. It can be seen that all MCM-41 supports gave the similar intensity of XRD characteristic peaks consisting of a broad peak of amorphous silica around 20 to 30°.

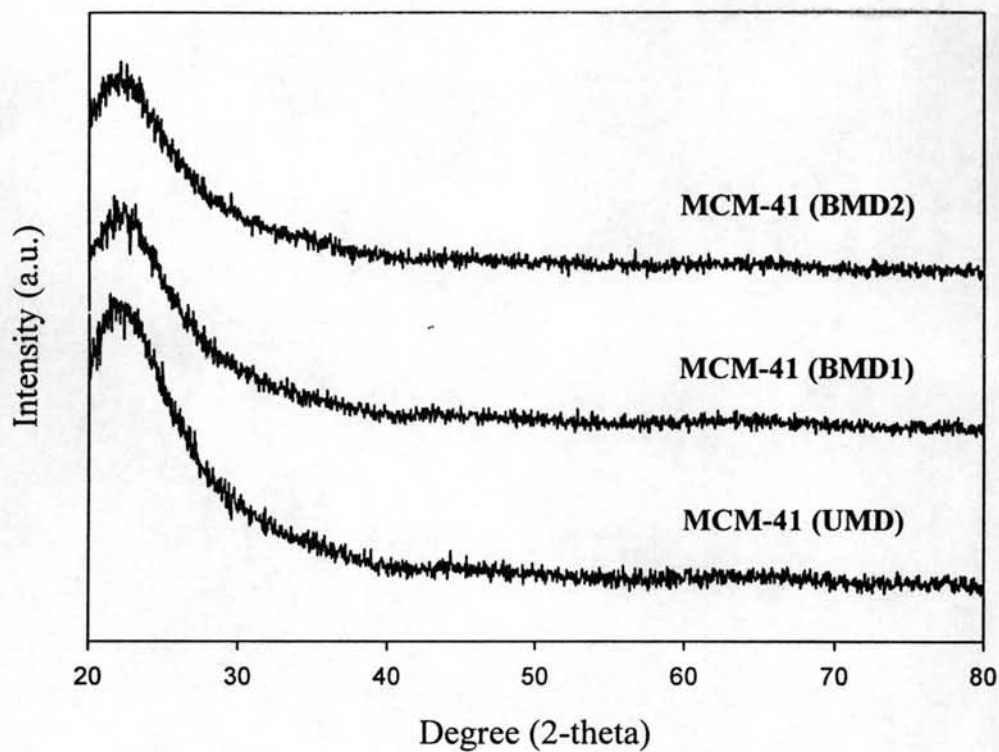


**Figure 4.2** XRD patterns of various MCM-41 supports

#### **4.1.3 Characterization of supports and catalyst precursors with raman spectroscopy**

As confirmation, no significantly different Raman bands (**Figure 4.3**) were also observed for all MCM-41 supports within the Raman shift ranged between 200 and 1000  $\text{cm}^{-1}$ .

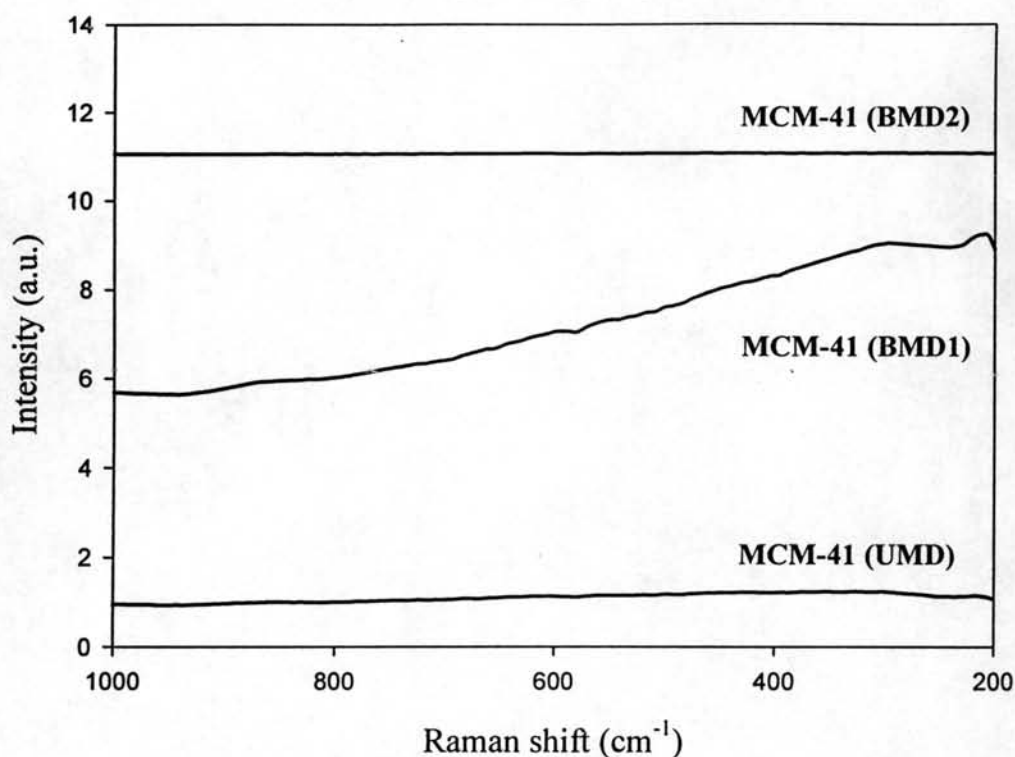


**Figure 4.3** Raman spectra of various MCM-41 supports

#### 4.1.4 Characterization of supports and catalyst precursors with x-ray photoelectron spectroscopy (XPS)

After impregnation with dMMAO, the nature and surface concentrations of  $[Al]_{dMMAO}$  on various MCM-41 supports were determined using the XPS measurement. The typical XPS profile (not shown) for all MCM-41-supported dMMAO exhibited the identical binding energy (BE) of Al 2p at ca. 74.6-74.7 eV. It should be noted that the BE for Al 2p obtained here was also in accordance with that on silica as reported by Hagimoto et al. [77]. Thus, it indicated that no transformation of the oxidation state for the cocatalyst (dMMAO) present on various MCM-41 supports employed. The surface concentrations of  $[Al]_{dMMAO}$  measured by XPS are also shown in **Table 4.2**. It can be observed that the surface concentrations of  $[Al]_{dMMAO}$  were similar for both MCM-41 (BMD) supports having  $[Al]_{dMMAO}$  at surface of 27.0 wt%. However, it appeared that the MCM-41 (UMD) support had a

slightly higher amount of  $[Al]_{dMMAO}$  at surface (27.3 wt%) than that of the MCM-41 (BMD) support. Besides the amounts of  $[Al]_{dMMAO}$  surface concentration, one should consider the distribution of the cocatalyst on the various supports.

**Table 4.2** XPS results for different supports

Support	BE for Al 2p <sup>a</sup> (eV)	Mass Concentration (%) of Al
dMMAO/MCM-41(UMD)	74.7	27.3
dMMAO/MCM-41(BMD1)	74.6	27.0
dMMAO/MCM-41(BMD2)	74.7	27.0

<sup>a</sup> Al 2p from dMMAO

#### 4.1.5 Characterization of supports and catalyst precursors with scanning electron microscope (SEM) and energy dispersive x-ray spectroscopy (EDX)

In order to determine the morphologies of the supports and elemental distributions of the supports after impregnation, SEM and EDX were performed, respectively. The SEM micrographs of various MCM-41 supports before impregnation with dMMAO are shown in **Figure 4.4**. It showed that surface of MCM-41(UMD) was more roughish than both MCM-41(BMD) and similar surface in both MCM-41(BMD). It was also in accordance with N<sub>2</sub> physisorption measurement, the MCM-41(BMD1) support having surface area 400.3 m<sup>2</sup>/g whereas the MCM-41(BMD2) having surface area 400.0 m<sup>2</sup>/g as also shown in **Table 4.1**, the result indicated that both bimodal MCM-41 gave similar surface area.

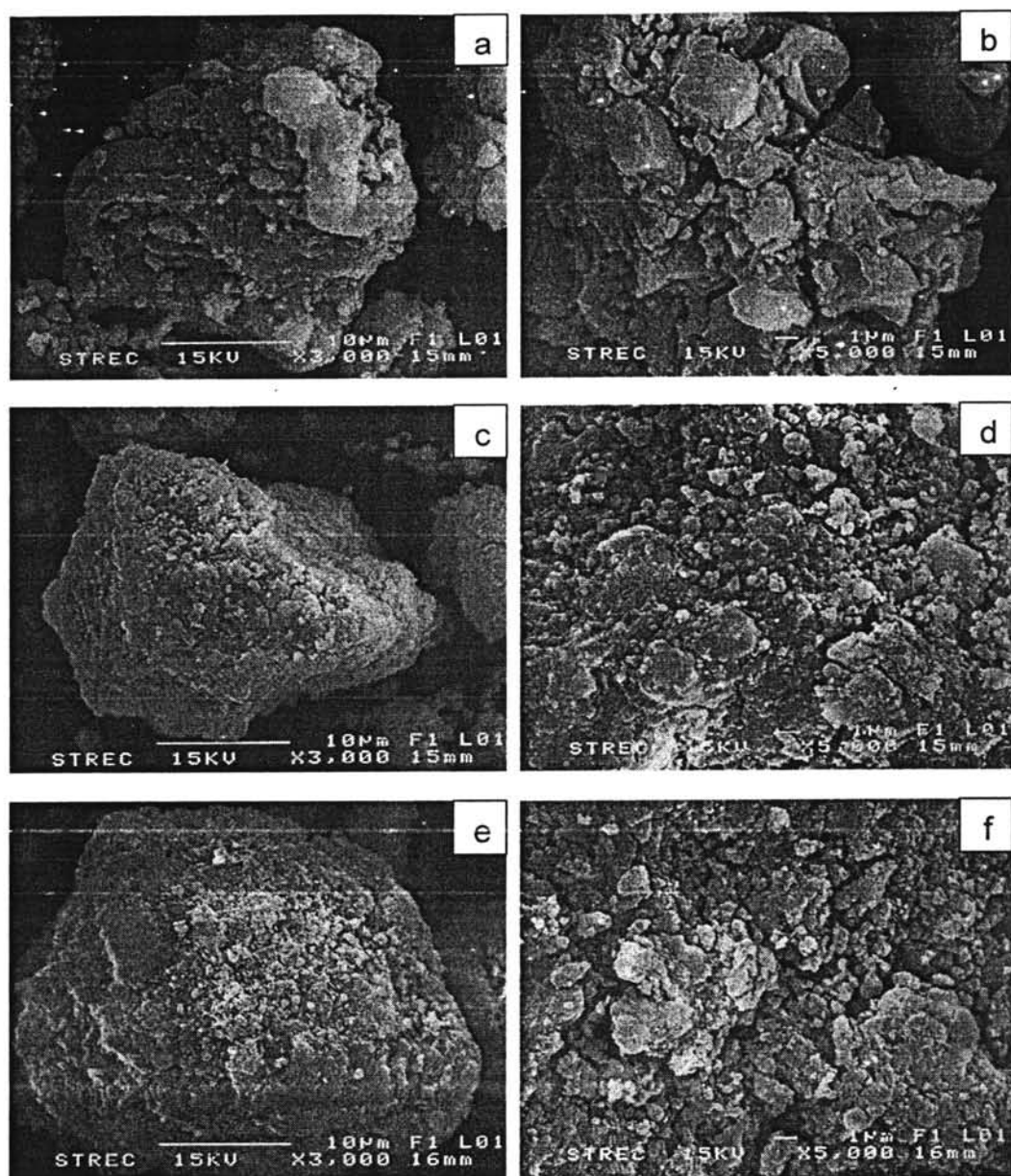


**Figure 4.4** SEM micrographs of various MCM-41 supports; a and b: MCM-41(UMD), c and d: MCM-41(BMD1), e and f: MCM-41(BMD2)

Therefore, the elemental distribution for  $[Al]_{dMMAO}$  was also performed using EDX mapping on the external surface of the catalyst precursors (as shown in appendix F). The  $[Al]_{dMMAO}$  distribution on various supports is shown in **Figure 4.5**. As seen, all samples exhibited good distribution of Al without any changes in the support morphology.

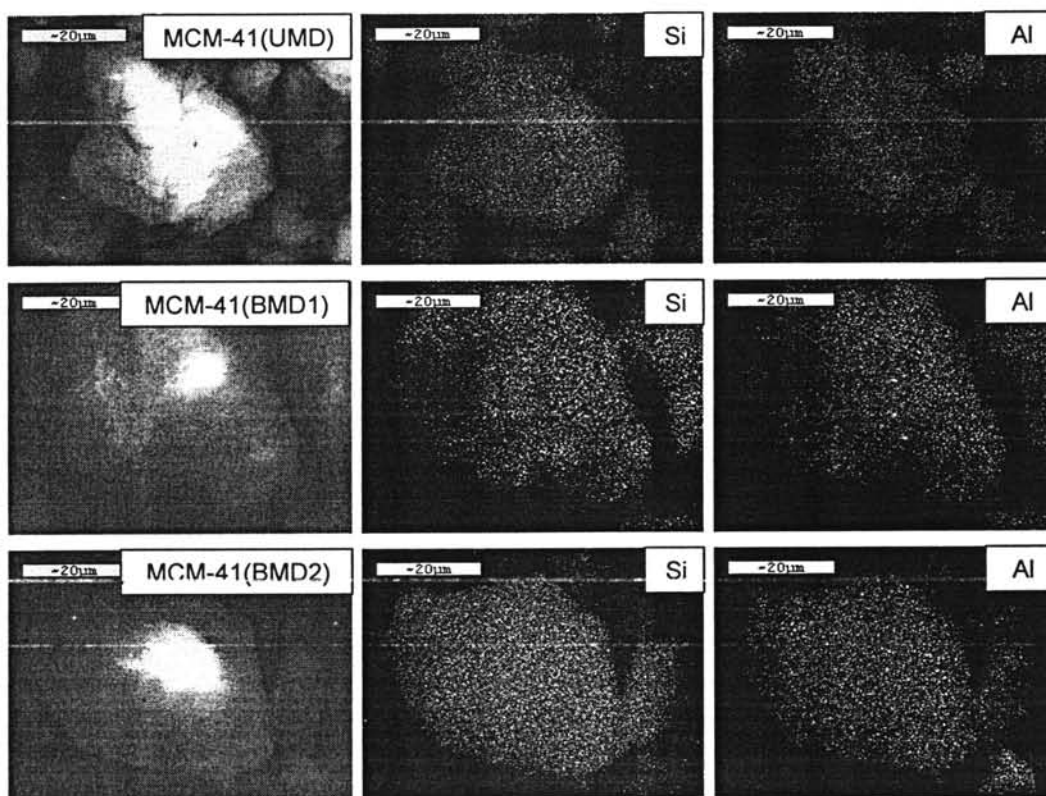


**Figure 4.5** EDX mapping of various MCM-41 supports after dMMAO impregnation

## 4.2 Effect of various MCM-41 supports in ethylene/1-octene copolymerization system

### 4.2.1 The effect of various MCM-41 supports on the catalytic Activity

The catalytic activities via various MCM-41 supports and the homogeneous system are listed in **Table 4.3**.

**Table 4.3** Catalytic activities of various MCM-41-supported dMMAO with zirconocene catalyst during ethylene/1-octene copolymerization

System	Polymerization time (s)	Polymer yield <sup>a</sup> (g)	Catalytic activities <sup>b</sup> ( $\times 10^{-4}$ kg Pol.mol.Zr <sup>-1</sup> .h <sup>-1</sup> )
Homogeneous	87	1.59	4.38
MCM-41(UMD)	186	1.58	2.04
MCM-41(BMD1)	127	1.58	2.99
MCM-41(BMD2)	150	1.51	2.42

<sup>a</sup> The polymer yield was fixed [limited by ethylene fed and 1-octene used (0.018 mole equally)].

<sup>b</sup> Activities were measured at polymerization temperature of 343 K, [Ethylene] = 0.018 mole,  $[Al]_{dMMAO} / [Zr]_{cat} = 1135$ ,  $[Al]_{TMA} / [Zr]_{cat} = 2500$ , in toluene with total volume = 30 ml and  $[Zr]_{cat} = 5 \times 10^{-5}$  M.

It was obvious that the homogeneous catalytic system provided the highest activity among the supported system due to the absence of supporting effect [78-80]. Considering the various MCM-41-supported systems, it was found that the MCM-41 (BMD) rendered higher activity than the UMD one about 1.2-1.5 times. Although the amount of  $[Al]_{dMMAO}$  at surface of the MCM-41 (UMD) as measured by XPS was slightly higher, the catalytic activity was lower. It is known that besides the concentrations of active species, one should consider on the interaction between the active species and support. In fact, too strong interaction can result in compound formation at surface [81-85] and/or inactive species leading to low catalytic activity. A wide range of variables including nature of supports and active species, particle size, and treatment conditions can affect the degree of support interaction. Essentially, they can be superimposed on each other. However, based on this study, the active species ( $[Al]_{dMMAO}$ ) present on different MCM-41 supports had the similar characteristics of Al 2p as measured by XPS indicating that no other compound formation on surface was formed. Thus, it was suggested that based on the similar amount of  $[Al]_{dMMAO}$  added, the size of the  $[Al]_{dMMAO}$  present in the small pore [MCM-41 (UMD)] was presumably smaller due to larger surface area. As a matter of fact, the smaller particle can interact more with the support resulting in stronger



support interaction. In order to identify the interaction of  $[Al]_{dMMAO}$  on various MCM-41 supports, the TGA measurement was performed. The TGA profiles of  $[Al]_{dMMAO}$  on various MCM-41 supports are shown in **Figure 4.6** indicating the similar profiles for various supports. It was observed that the weight loss of  $[Al]_{dMMAO}$  present on various supports were in the order of MCM-41 (BMD1) (12.8%) > MCM-41 (BMD2) (12.2%) > MCM-41 (UMD) (11.5%). Based on TGA, it indicated that the  $[Al]_{dMMAO}$  present on MCM-41 (UMD) had the strongest interaction among the other supports, thus, having the lowest polymerization activity. It is worth noting that the higher activity obtained from the bimodal support can be attributed to the optimum interaction between the support and active species.

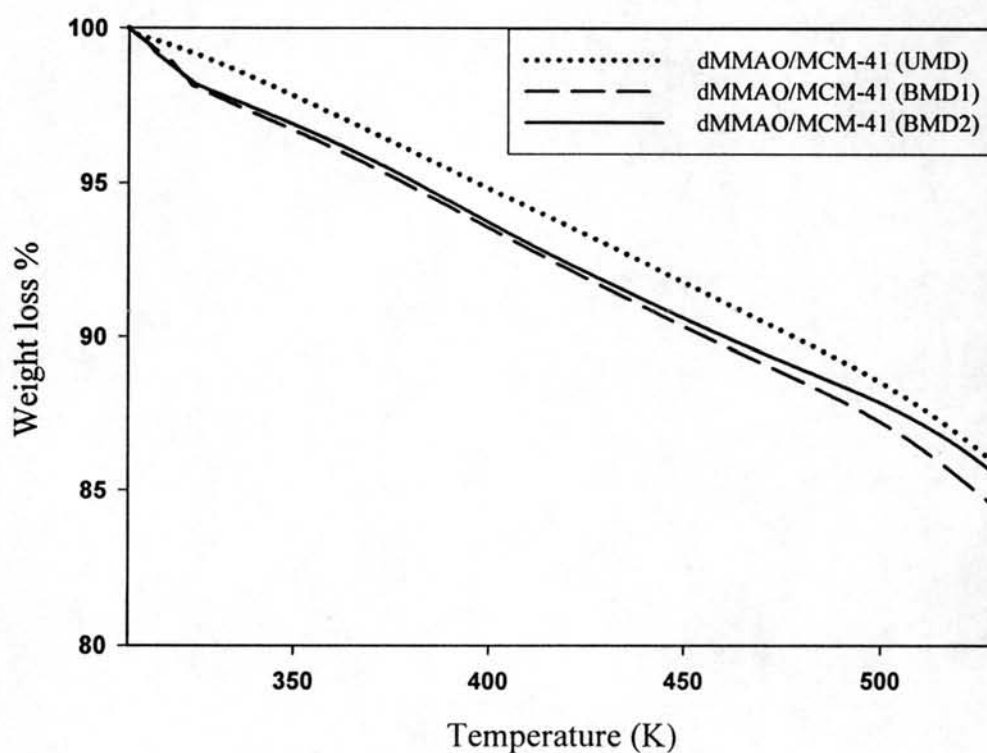


**Figure 4.6** TGA profiles of  $[Al]_{dMMAO}$  on various MCM-41 supports

#### 4.2.2 The effect of various MCM-41 supports on the molecular weight of copolymers

The various copolymers obtained were further characterized by means of GPC and  $^{13}\text{C}$  NMR. The GPC was performed in order to determine the MW,  $M_n$  and MWD of polymers. The GPC results are shown in **Table 4.4**. Considering the different catalytic systems, it can be observed that the homogeneous system exhibited higher MW than the supported system did. As known from our previous works, the supported system apparently promoted the chain transfer reaction resulting in lower MW of polymers [79,86]. Based on the supported system, it revealed that the copolymer obtained from the bimodal MCM-41 supports had broader MWD than that derived from the unimodal one. It was suggested that this broad MWD copolymer can be attributed to the different natures of catalytic sites present on the bimodal supports. However, the observed MW of copolymers among all supports was slightly different.

**Table 4.4** Molar weight (MW) and molecular weight distribution (MWD) of polymers obtained from various MCM-41-supported dMMAO with zirconocene catalyst

System	MW <sup>a</sup> ( $\times 10^{-4}$ g mol <sup>-1</sup> )	$M_n$ <sup>a</sup> ( $\times 10^{-4}$ g mol <sup>-1</sup> )	MWD <sup>a</sup>
Homogeneous	3.66	0.69	5.3
MCM-41(UMD)	2.91	0.98	3.0
MCM-41(BMD1)	2.69	0.45	6.0
MCM-41(BMD2)	3.07	0.62	5.0

<sup>a</sup> Obtained from GPC and MWD was calculated from MW/ $M_n$

#### 4.2.3 The effect of various MCM-41 supports on the melting temperatures of copolymers

The melting temperatures ( $T_m$ ) of copolymer were evaluated by the differential scanning calorimeter (DSC) are shown in **Table 4.5**. DSC curves of the copolymer are also shown in Appendix B

**Table 4.5** Melting temperatures of copolymers obtained various MCM-41 supports

Systems	$T_m(^{\circ}\text{C})$	% crystallinity
Homogeneous	n.o.	1.36
MCM-41(UMD)	n.o.	n.o.
MCM-41(BMD1)	94.6	1.76
MCM-41(BMD2)	n.o.	n.o.

n.o. refers to not observe

From the characterization of copolymer in **Table 4.5**, it appeared only the melting temperatures ( $T_m$ ) of copolymer obtained from the MCM-41(BMD1) support. The absence of  $T_m$  for copolymers obtained from other supports can be probably due to higher degree of 1-octene incorporation.

#### 4.2.4 The effect of various MCM-41 supports on the incorporation of copolymers

The quantitative analysis of triad distribution for all copolymers was conducted on the basis assignment of the  $^{13}\text{C}$  NMR spectra of ethylene/1-octene (EO) copolymer and calculated according to the method of Randall [87]. The characteristics of  $^{13}\text{C}$  NMR spectra (as shown in appendix C) for all copolymers were similar indicating the copolymer of ethylene/1-octene. The triad distribution of all polymers is shown in **Table 4.6**. Ethylene incorporation in all systems gave copolymers with similar triad distribution. It was also shown a little probability to produce the block of OO, which is the characteristic of this zirconocene in homogeneous system [78]. No triblock of OOO in the copolymers was found. Only the random copolymers can be produced in all systems. In addition, the octene incorporations in all supported systems were between 21 and 29 mol%, which was similar with that in the homogeneous system.

**Table 4.6**  $^{13}\text{C}$  NMR analysis of ethylene/1-octene copolymer

System	Triad distribution of copolymer						Mol % of O in copolymer
	OOO	EOO	EOE	EEE	OEO	OEE	
Homogeneous	0	0.077	0.177	0.468	0.052	0.226	25
MCM-41(UMD)	0	0.084	0.208	0.519	0.054	0.136	29
MCM-41 (BMD1)	0	0.085	0.190	0.483	0.049	0.193	27
MCM-41 (BMD2)	0	0.054	0.152	0.510	0.050	0.234	21

E refers to ethylene monomer and O refers to 1-octene comonomer

**Table 4.7** Reactivity ratios of ethylene and 1-octene monomer

System	$r_{E/O}$
Homogeneous	0.62
MCM-41(UMD)	0.71
MCM-41 (BMD1)	0.69
MCM-41 (BMD2)	0.57

E refers to ethylene monomer and O refers to 1-octene comonomer

### 4.3 The effect of various MCM-41 supports with different comonomers

#### 4.3.1 The effect of various MCM-41 supports with different comonomers on the catalytic activity

Then, the various MCM-41 supports after impregnation with dMMAO were used and investigated for catalytic activities upon various comonomers employed (1-hexene, 1-octene and decene). Copolymerization of ethylene/1-hexene and ethylene/1-decene with various MCM-41-supported dMMAO with zirconocene catalyst was performed in order to determine the catalytic activities influenced by the

various supports and comonomers. Dried Modified methylaluminoxane (dMMAO) was used as cocatalyst which the molar ratio of Al<sub>(MAO)</sub>/Zr was 1135. The copolymerizations were performed in toluene solvent at 70°C using ethylene

consumption of 0.018 mol (pressure in reactor 50 psi), 0.018 ml of  $\alpha$ -olefin, 100 mg of catalyst precursor and zirconium concentration  $5.0 \times 10^{-5}$  M with total solution volume of 30 ml. The resulted reaction study is shown in **Table 4.8**.

**Table 4.8** Catalytic activities of various MCM-41-supported dMMAO with zirconocene catalyst during ethylene/ $\alpha$ -olefin copolymerization

Comonomer	System	Polymerization time (s)	Polymer yield <sup>a</sup> (g)	Catalytic activities <sup>b</sup> ( $\times 10^{-4}$ kg Pol. mol.Zr <sup>-1</sup> .h <sup>-1</sup> )
1-Hexene	Homogeneous	98	1.58	3.87
	MCM-41(UMD)	152	1.52	2.4
	MCM-41(BMD1)	127	1.53	1.69
	MCM-41(BMD2)	150	1.53	1.68
1-Octene	Homogeneous	87	1.59	4.38
	MCM-41(UMD)	186	1.58	2.04
	MCM-41(BMD1)	127	1.58	2.99
	MCM-41(BMD2)	150	1.51	2.42
1-Decene	Homogeneous	154	1.55	2.42
	MCM-41(UMD)	143	1.51	2.53
	MCM-41(BMD1)	113	1.57	3.33
	MCM-41(BMD2)	127	1.54	2.91

<sup>a</sup> The polymer yield was fixed [limited by ethylene fed and 1-olefins used (0.018 mole equally)].

<sup>b</sup> Activities were measured at polymerization temperature of 343 K, [Ethylene] = 0.018 mole, [Al]<sub>dMMAO</sub> / [Zr]<sub>cat</sub> = 1135, [Al]<sub>TMA</sub> / [Zr]<sub>cat</sub> = 2500, in toluene with total volume = 30 ml and [Zr]<sub>cat</sub> =  $5 \times 10^{-5}$  M.

For copolymerization of ethylene with three different comonomers, it was obvious that the homogeneous catalytic system provided the highest activity among the supported system due to the absence of supporting effect, except for the the

ethylene/1-decene (ED) copolymerization where the bimodal MCM-41 supports catalyst exhibited much higher catalytic activity than the homogeneous system. However, considering only the supported system, it was found that bimodal MCM-41 had lower catalytic activity for ethylene/1-hexene (EH) copolymerization and higher catalytic activity for ethylene/1-octene (EO) and ED copolymerization. The maximum activity of all comonomers can be obtained with the presence of MCM-41(BMD1) support for EO and ED copolymerization.

#### 4.3.2 The effect of various MCM-41 supports with different comonomers on the molecular weight of copolymer

The molecular weight based on weight average ( $M_w$ ) and based on number average ( $M_n$ ), and molecular weight distribution (MWD) of polymers obtained by a gel permeation chromatography are shown in **Table 4.9** and GPC curves of the copolymer are also shown in appendix A.

**Table 4.9** Molar weight (MW) and molecular weight distribution (MWD) of copolymers obtained from various MCM-41-supported dMMAO with zirconocene catalyst

Comonomer	System	MW <sup>a</sup> ( $\times 10^{-4}$ g mol <sup>-1</sup> )	$M_n^a$ ( $\times 10^{-4}$ g mol <sup>-1</sup> )	MWD <sup>a</sup>
1-Hexene	Homogeneous	3.44	1.01	3.4
	MCM-41(UMD)	4.05	0.54	7.5
	MCM-41(BMD1)	3.24	0.64	5.1
	MCM-41(BMD2)	3.55	0.63	5.6
1-Octene	Homogeneous	3.66	0.69	5.3
	MCM-41(UMD)	2.91	0.98	3.0
	MCM-41(BMD1)	2.69	0.45	6.0
	MCM-41(BMD2)	3.07	0.62	5.0
1-Decene	Homogeneous	4.31	0.68	6.3

	MCM-41(UMD)	5.24	0.6	8.7
	MCM-41(BMD1)	3.51	0.51	6.9
	MCM-41(BMD2)	5.45	0.9	6.1

<sup>a</sup> Obtained from GPC and MWD was calculated from  $MW/M_n$

For copolymers of ethylene with different comonomers, considering EH and ED copolymerization, it was found that unimodal MCM-41 resulted in decreased molecular weight and gave the broader molecular weight distribution of copolymer compared to bimodal, it was contrary results with the polymer obtained with EO copolymerization.

#### 4.3.3 The Effect of various MCM-41 supports on the melting temperatures of copolymers with different comonomers

The melting temperatures ( $T_m$ ) of copolymer were evaluated by differential scanning calorimeter (DSC) and are shown in **Table 4.10**. DSC curves of the copolymer are also shown in Appendix B.

**Table 4.10** Melting temperatures % crystallinity of copolymers using various MCM-41 supports with different comonomer

Comonomer	Systems	$T_m(^{\circ}C)$	% crystallinity
1-Hexene	Homogeneous	n.o.	n.o.
	MCM-41(UMD)	70.3	n.o.
	MCM-41(BMD1)	n.o.	n.o.
	MCM-41(BMD2)	n.o..	n.o.
1-Octene	Homogeneous	n.o.	n.o.
	MCM-41(UMD)	n.o.	n.o.
	MCM-41(BMD1)	94.6	n.o.
	MCM-41(BMD2)	n.o.	n.o.
1-Decene	Homogeneous	n.o.	n.o.
	MCM-41(UMD)	82.1	1.43
	MCM-41(BMD1)	93.8	n.o.
	MCM-41(BMD2)	85.9	2.48

n.o. refers to not observe

From the characterization of copolymer in **Table 4.10**, it was found that, the melting temperatures ( $T_m$ ) of copolymer increased with the various MCM-41 supports. It was found ED and EH exhibited decreased  $\alpha$ -olefin incorporation with various MCM-41 supports.

#### **4.3.4 The effect of various MCM-41 supports on incorporation of copolymer the with different comonomers**

$^{13}\text{C}$  NMR spectroscopy was used to determine comonomer incorporation and polymer microstructure. The quantitative analysis of triad distribution for all copolymers was conducted and calculated according to the method of Randall. The result obtained for the triad sequence distribution of copolymer shown in **Table 4.11**. All copolymers were similar indicating the copolymer of EH EO and ED. It was not shown the block of HH and gave similar comonomer incorporation except in the MCM-41(BMD1) system. It was shown higher comonomer incorporation compared with other systems in same comonomer and no triblock of HHH and DDD in the copolymers was found.

In the ED copolymerization, ethylene incorporation in all systems gave copolymers with similar triad distribution. It was also shown a little probability to produce the block of DD. It was shown the higher comonomer incorporation compared with other systems with different comonomers. No triblock of DDD in the copolymers was found.

The result suggested that all copolymers had a random distribution of comonomer insertion with average amounts of comonomer triad in the polymer chain. Only the random copolymers can be produced in all systems, the hexene incorporations in all supported systems were between 19 and 23 mol% and the decene incorporations in all supported systems were between 21 and 33 mol%.



**Table 4.11**  $^{13}\text{C}$  NMR analysis of ethylene/ $\alpha$ -olefins copolymer

Comonomer	System	Triad distribution of copolymer						Mol % of C in copolymer
		HHH	EHH	EHE	EEE	HEH	HEE	
<b>1-Hexene</b>	Homogeneous	0	0	0.175	0.531	0.041	0.253	17
	MCM-41(UMD)	0	0	0.193	0.501	0.048	0.258	19
	MCM-41(BMD1)	0	0	0.232	0.432	0.077	0.259	23
	MCM-41(BMD2)	0	0	0.197	0.502	0.051	0.250	20
Comonomer	System	OOO	EOO	EOE	EEE	OEO	OEE	
<b>1-Octene</b>	Homogeneous	0	0.077	0.177	0.468	0.052	0.226	25
	MCM-41(UMD)	0	0.084	0.208	0.519	0.054	0.136	29
	MCM-41(BMD1)	0	0.085	0.190	0.483	0.049	0.193	27
	MCM-41(BMD2)	0	0.054	0.152	0.510	0.050	0.234	21
Comonomer	System	DDD	EDD	EDE	EEE	DED	DEE	
<b>1-Decene</b>	Homogeneous	0	0.104	0.246	0.304	0.090	0.256	35
	MCM-41(UMD)	0	0.054	0.185	0.462	0.077	0.223	24
	MCM-41(BMD1)	0	0.079	0.252	0.279	0.127	0.263	33
	MCM-41(BMD2)	0	0.010	0.195	0.565	0.008	0.222	21

E refers to ethylene monomer and C refers to H (1-hexene), O (1-octene) and D (1-decene) comonomer

**Table 4.12** Reactivity ratios of ethylene and  $\alpha$ -olefin monomers

Comonomer	Systems	$r_E r_H$
1-Hexene	Homogeneous	0
	MCM-41(UMD)	0

	MCM-41(BMD1)	0
	MCM-41(BMD2)	0
<b>Comonomer</b>	<b>Systems</b>	<b>r<sub>E</sub>r<sub>O</sub></b>
1-Octene	Homogeneous	0.62
	MCM-41(UMD)	0.71
	MCM-41(BMD1)	0.69
	MCM-41(BMD2)	0.57
<b>Comonomer</b>	<b>Systems</b>	<b>r<sub>E</sub>r<sub>D</sub></b>
1-Decene	Homogeneous	0.34
	MCM-41(UMD)	0.39
	MCM-41(BMD1)	0.21
	MCM-41(BMD2)	0.14

E refers to ethylene monomer and C refers to H (1-hexene), O (1-octene) and D (1-decene) comonomer